analytical chemistry

Article

pubs.acs.org/ac

Accuracy of Ion Mobility Measurements Dependent on the Influence of Humidity

Thomas Mayer and Helko Borsdorf*

UFZ—Helmholtz Centre for Environmental Research Leipzig-Halle, Department Monitoring and Exploration Technologies, Permoserstraße 15, D-4318 Leipzig, Germany

ABSTRACT: Measurements with sensor techniques in field analytical chemistry can be considerably affected by varying ambient conditions such as humidity. We systematically investigated the way in which ion mobility measurements are influenced by moisture. Both the peak positions of product ions within the spectrum and their relative abundance can vary depending on humidity. The transportation of humidity via the carrier gas into the ion mobility spectrometer causes changes in ionization pathways. Additional reactant ion species are formed and a lower relative abundance of product ions from halogenated compounds was generally observed. The peak position within the ion mobility spectrum is comparatively unaffected for the same ions. In contrast, considerable differences in drift times detected were found with increasing humidity of drift gas, while the influence on calibration was not as significant for chlorinated and brominated substances as observed for humid carrier gases.

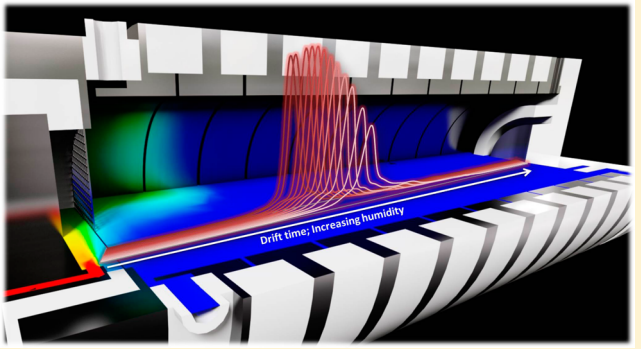

Ion mobility spectrometry (IMS) is a well-established sensor technique for detecting chemical warfare agents,[1] environmental pollution,[2] and industrial chemicals.[3] Furthermore, its application in clinical diagnostic purposes,[4,5] pharmacy,[6−8] biomedical science,[9] as explosive detectors in airports worldwide[10−12] and in monitoring the cabin atmosphere onboard the International Space Station[13] has been described in detail in the relevant literature.[14]

Ion mobility measurements are based on drift velocities (v_d) of ion swarms derived from sample molecules.[15] Since the measurements are made on ions, the formation of these ions from neutral sample molecules is a first and controlling event in this method. Ionization of samples also occurs in air at ambient pressure. The most commonly used method for ionization in conventional ion mobility analysis is via chemical reactions between sample and reactant ions that are created by the emission of electrons from radioactive nickel (^{63}Ni) or tritium (^{3}H) into a supporting atmosphere. In conventional time-of-flight methods, ions are injected at a given time interval of a few microseconds via an electronic shutter into the drift region. In this region with typical lengths ranging between 5 and 15 cm, the ion packet moves as a swarm toward a detector down a voltage gradient and through a gas flow, either air or nitrogen. This drift gas flows in a direction opposite to that of ion motion and has typical flow rates of a few hundred mL min^{-1}. Swarm velocities in electric fields of 300 V cm^{-1} are often 2 m s^{-1} so a spectrum is generated every 5 to 25 ms. Drift velocity may be associated with the ion structure or identity through mass, charge and collision cross sections, which are in turn derived from structural parameters of size, shape, and the charge location or distribution. The ion swarm has characteristic drift velocities, which provide the basis for ion separation through differences in mass and structure.[16,17]

Historically, a key advantage of IMS has been the ability to perform high speed on-site measurements using hand-held or transportable instruments. The results are available within a few minutes with high information density and excellent detection limits. Ion mobility measurements provide confidence in measurements from spectra which are characteristic for certain substances. Other sensors such as photoionization detectors, surface acoustic wave sensors or electronic noses are less expensive than IMS analyzers and normally provide sum signals. In comparison, IMS provides a higher level of quantitative and qualitative detail in a measurement.[18]

As generally known from experience using field-deployable sensor techniques, measurements are often influenced by the sample matrix. Furthermore, the measuring conditions in field analytical chemistry (e.g., humidity and environmental temperature) can vary considerably in comparison to the analysis in the lab.[19,20]

While the influence of temperature[21−23] and pressure[24−26] on ion formation and drift behavior in IMS have been investigated for several classes of substances, there is a lack of in-depth knowledge regarding the qualitative and quantitative influence of humidity on the ion mobility spectra. Although the first pioneering paper about the effects of water vapor on mobility of gaseous ions was published as far back as 1928,[27] only a few investigations have been undertaken with modern

Received: February 25, 2014
Accepted: April 8, 2014
Published: April 9, 2014

   dx.doi.org/10.1021/ac5007393 | *Anal. Chem.* 2014, 86, 5069−5076

ion mobility spectrometers. Vautz et al. investigated terpenes with photoionization and observed decreased signal intensities with increasing carrier gas humidity.[28,29] The composition of reactant ions and negative chlorinated product ions was investigated by coupling a membrane inlet ion mobility spectrometer with ^{63}Ni ionization and mass spectrometry.[30] To simulate the aging of filter media, water was added to the adsorbent traps. No changes were observed for the composition of product ions with increasing humidity, while reduced sensitivity was found and the peaks appeared at higher drift times. Positive product ions of triethylamine dependent on humidity were studied with IMS using a ^{63}Ni ionization source.[31] While detection sensitivity in this case is to a certain extent dependent on humidity, considerable differences were observable for peak position and shape. The limited number of investigations surprises because the importance of moisture (in addition to temperature) on IMS measurements was identified as the most significant parameter which can hardly be overstated.[32]

Ion mobility spectrometers are typically applied in two preferred configurations. A membrane inlet in combination with an internal gas circuit for the drift gas is often used. Membrane inlets are particularly valuable as they prevent excessive interactions with moisture from ambient air. The moisture content of the carrier gas, which transports the sample into the ionization region, is therefore minimally influenced by atmospheric humidity. On the other hand, the detection limits are much higher in comparison with a direct sample inlet. Although a membrane inlet normally preserves the purity of the internal atmosphere, frequent measurements in a humid environment can lead to an accumulation of humidity within the drift gas of the internal gas circuit.

To improve detection limits, spectrometers with a direct sample inlet and external gas supply are used. In contrast to the aforementioned configuration, the drift gas remains comparatively unaffected by atmospheric humidity, while the carrier gas transports the ambient humidity directly to the ion source. The amount of humidity within the ion source in this case depends on the ratio between carrier gas flow (usually 20−100 mL min^{-1}) and drift gas flow (usually 400−600 mL min^{-1}) as well as on the duty cycle of sample introduction.

On the basis of these two configurations, we systematically investigated the influence of humidity in carrier and drift gases on both the peak position within the ion mobility spectrum and quantification. The investigations were performed with commonly used beta emitting radiation sources. Because of the practical necessity to interpret sensor data, quantitative data were determined and are presented here for the first time. Significant technical challenges that arose were the controlled introduction of the carrier gas with a defined concentration of analytes and defined humidity levels, as well as the adjustment of the moisture content of our drift gas.

Halogenated substances were used as target compounds due to their importance when used for detecting environmental pollution, industrial chemicals or blister agents. 1-Chlorohexane, 1-bromohexane, and 1-iodohexane were investigated as examples of compounds that have comparable structure to each other and yet different substituents, while trichloroethene and benzyl chloride, in addition to 1-chlorohexane, are chlorinated substances with different structural features. Using beta emitting radiation sources, all of these compounds form negative product ions $(H_2O)nX^-$ because of dissociative charge transfer reactions. The resulting spectra are therefore well-defined with one major product ion peak.[33]

EXPERIMENTAL SECTION

Sample Introduction System. Samples were introduced via permeation tubes. Three hundred microliters of the neat sample was sealed in polyethylene permeation tubes which were placed in a temperature-controlled glass column. Nitrogen (5.0 grade quality with moisture content of up to 5 ppm) was passed through the glass column with a flow rate of 500 mL min^{-1}. This flow rate was kept constant for approximately 8 h as the substances passed through the permeation vessel. Using a needle valve and controlling flow with a mass flow meter (Analyt, Müllheim, Germany), the sample gas stream was split and a portion of flow was guided into a mixing chamber. Here, the sample gas stream can be additionally diluted by two mass flow controllers with a range of 0−500 mL min^{-1} (Analyt, Müllheim, Germany). An aliquot of this diluted sample gas stream is transported into a second mixing chamber via a rotary vane pump (model G12/01EB, GD Thomas, Puchheim, Germany). The second mixing chamber permits the additional dilution of the sample gas with nitrogen and its subsequent humidification. The gas stream for humidification is generated by mixing gas flows with 0% and 100% relative humidity. The saturated gas flow was generated by a bubble saturator. The gas stream bubble up through liquid water. The water used for this procedure was purchased from Merck (Darmstadt, Germany) in LC-MS grade. Both gas flows can be adjusted with needle valves. The resulting gas flow into the mixing chamber is also controlled by a mass flow meter. The carrier gas stream that flows into the IMS was then taken from this mixing chamber via a rotary vane pump (95 mL min^{-1}). The humidity of this final gas flow was monitored with an AMX1 moisture sensor (Panametrics, Hofheim, Germany). All mass flow meters and mass flow controllers were calibrated with a bubble meter before use. The data acquisition was started if a constant level of moisture was achieved.

The concentration of the compounds in the sample gas stream was calculated using the weight loss of the permeation tube over a certain time considering the total gas throughput. Before weighting, the samples were prepermeated for equilibration of the permeation rate for a few hours. Each series of measurements was performed at least three times. An advantage of such a system is the opportunity for adjusting a broad range of concentrations and levels of humidity within a series of measurements. However, this approach requires a careful optimization of the experimental design to ensure adjustable flow rates and to avoid potential overpressurization.

For humidification of drift gas, this introduction system was separated. The sample gas stream was generated in the first mixing chamber while the drift gas was produced in the second mixing chamber. Instead of nitrogen, synthetic air was used for generating drift gas.

Ion Mobility Measurements. An experimental setup based on a commercially available ion mobility spectrometer (STEP Sensortechnik and Elektronik Pockau GmbH, Pockau, Germany) was used. The device is equipped with a tritium ionization source (50 MBq). A metallic grid separates the ion source from the drift region. It is located approximately 2 mm away from the ion source and has the same potential as the first drift ring. The ions formed are gated to the drift tube via an 80 μs impulse, which is applied to the ion source (approximately 400 V more negative in comparison to the metallic grid). The

dx.doi.org/10.1021/ac5007393 | Anal. Chem. 2014, 86, 5069−5076

drift tube has a traditional stacked ring electrode design with a length of 56 mm between the inlet grid and aperture grid, which is positioned 0.7 mm in front of the faraday plate. The inner diameter of the drift region is 18 mm. The ring electrodes are made from stainless steel, the isolators from PEEK. An electric field of approximately 300 V cm^{-1} is created by resistive voltage dividers. System temperature remained constant at 80 °C. Carrier gas and drift gas were externally supplied from the described introduction system. Nitrogen with a flow rate 95 mL min^{-1} was generally used as a carrier gas, while the drift gas was synthetic air with a flow rate of 550 mL min^{-1}. The spectrometer has a bidirectional flow system. The samples are introduced via the carrier gas directly on the surface of ion source, while the drift gas inlet is at the end of the drift tube. The gas outlet is positioned approximately 3 mm away from the ion source. Data acquisition and spectra analysis were performed using IMS Control Basic software (STEP Sensortechnik and Elektronik Pockau GmbH, Pockau, Germany). All measurements were recorded using negative polarity in order to detect negative ions.

RESULTS AND DISCUSSION

General. In the first step, we considered the flow conditions and distribution of humidity within the ion mobility spectrometer. Figure 1 shows the results of computational fluid dynamic (CFD) calculations. Initially, a three-dimensional CAD model of our experimental setup was created with Autodesk Inventor (Autodesk, San Rafael, U.S.A.). This model was imported to the Autodesk Simulation CFD program (Autodesk, San Rafael, U.S.A.). The boundary conditions used correspond to the parameters described in the Experimental Section. The calculations were carried out for two settings: (1) during the introduction of the humid carrier gas (793 ppm water content) and dry drift gas (9 ppm), as well as (2) dry carrier gas (9 ppm) and humid drift gas (793 ppm) were introduced (Figure 1A and C). The blue color indicates the humid gas while the red one represents the dry gas. In both cases, the humidity of the drift gas is homogeneously distributed within the complete drift tube and is mainly affected by the original drift gas humidity levels. More significant differences can be observed in the ionization region. Figure 1B shows the humidity levels along the ion source. The sample inlet in our spectrometer is positioned at the edge of the ion source. The sample gas stream is directly guided over the surface of the ion source, which is configured as a disk. Figure 1B shows the humidity level 0.2 mm above the surface along the diameter (12 mm). The humidity in this region is significantly higher in the case of the humid carrier gas. Although the flow rate of the drift gas is much higher in comparison to the carrier gas, its influence on humidity within the ion source is lower.

The chemical processes within the ion source are based on interaction between the reactant ions and analyte molecules. The degree of clustering (n) of $(H_2O)_nO_2^-$ reactant ions and $(H_2O)_nX^-$ product ions (where X^- is Cl^-, Br^-, and I^-) varies with changes in humidity. The degree of clustering that is dependent on moisture and temperature can be calculated using known enthalpies ($\Delta H°$) and entropies ($\Delta S°$) of hydration. The thermodynamic data used comes from the Chemistry Webbook (http//webbook.nist.gov/). The free-energy changes ($\Delta G°$) and equilibrium constants (K) at temperature (T) for each addition of water molecules were then evaluated using the equations

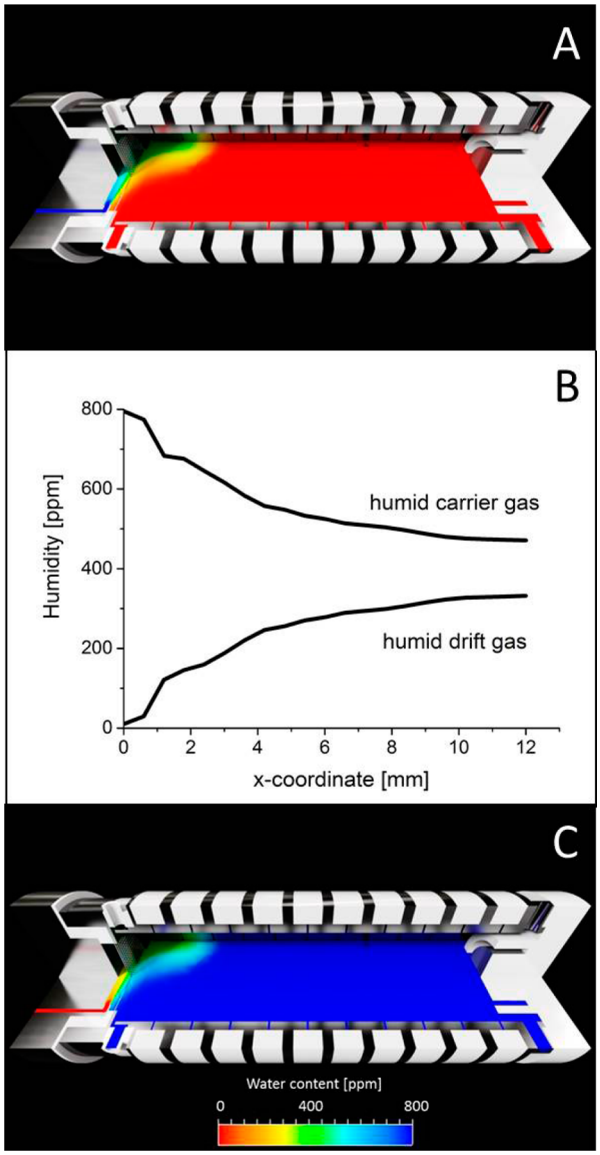

Figure 1. Flow conditions and humidity distribution within the ion mobility spectrometer with (A) humid carrier gas (793 ppm moisture) and dry drift gas (9 ppm) and (C) dry carrier gas (793 ppm) and humid drift gas (9 ppm). The distribution of humidity in the reaction region is shown in panel B. The X-coordinate represents the distance from the sample inlet across the ion source, which is formed as a disk.

$$\Delta G° = \Delta H° - T\Delta S° \quad (1)$$

and

$$K = \exp\left(\frac{-G°}{RT}\right) \quad (2)$$

where R is the gas constant. The relative concentration of water clusters at a certain temperature and water partial pressure p_w (at a standard pressure p_0) can be calculated according to eq 3

$$[O_2^-(H_2O)_n] = K_0 \times K_1 \times \ldots \times K_n\left(\frac{p_w}{p_0}\right)^n \quad (3)$$

The approach used for this calculation is described in more detail in previous publications.[34−37] Although this procedure only permits rough approximation due to the variety of data available and numerous determination methods used, the

dx.doi.org/10.1021/ac5007393 | Anal. Chem. 2014, 86, 5069−5076

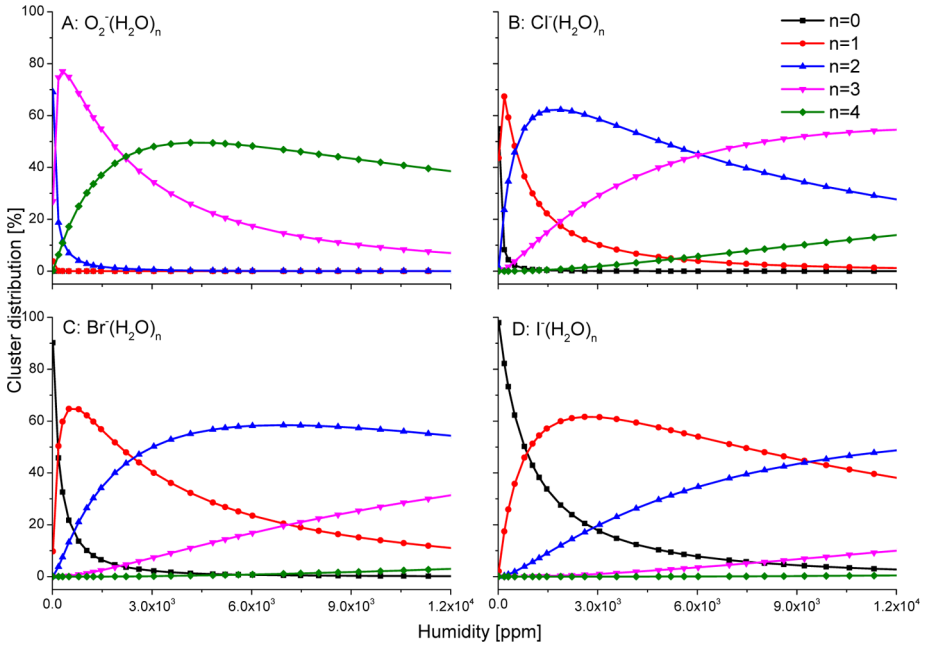

Figure 2. Calculated degree of clustering for negative reactant ions (A) and clustered halogenated product ions (B–D) depending on humidity at a constant temperature of 80 °C.

general trend of enhanced clustering with increasing humidity can be clearly identified. The results for the percentage distribution are summarized in Figure 2A for negative reactant ions and for product ions formed via dissociative electron attachment of halogenated compounds (shown in Figure 2B-2D). According to these calculations, $(H_2O)_2O_2^-$ reactant ions are predominantly found at humidity levels below 100 ppm, $(H_2O)_3O_2^-$ reactant ions between 100 and 2000 ppm, while mainly $(H_2O)_4O_2^-$ ions are mainly and preferentially formed above 2000 ppm humidity. The tendency to form water clusters made up from halogenated product ions decreases in the following order: chloride > bromide > iodide. While no unclustered product ions can be expected for chloride over the whole range of humidity, I^- is the predominant product ion up to a humidity of approximately 900 ppm.

Although the general behavior of ions can be concluded from these calculations, the transferability to experimental data is subject to many uncertainties. Electrons emitted from a Tritium source have typical current penetration of 2–3 mm. The detailed concentration of water on the surface of the ion source and its spatial distribution within the ionization region varies (see Figure 1). As such, the occurrence of parallel ionization reactions can therefore be expected depending on water concentration within the ionization space.

Our general findings regarding reactant ion chemistry, which is the basis for subsequent ionization reactions, are summarized in Figure 3. The spectra show the negative reactant ions without any sample depending on humidity of carrier gas (Figure 3A) or drift gas (Figure 3B). As can be seen, increasing carrier gas humidity causes the intensities of negative reactant ions to decrease and creates additional peaks. However, the main peak can be detected at the same drift time of 5.3 ms over the whole range of humidity. Two additional peaks with a sharp and symmetric profile appear at 6.1 and 7.0 ms, respectively, and are observable above 80 ppm humidity. Furthermore, additional ions can be seen at a drift time of 5.6 ms, as a shoulder of the main reactant ion peak. All of these peaks are

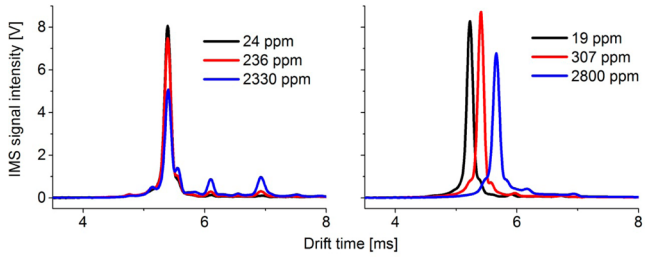

Figure 3. Negative ion mobility spectra without sample with (A) increasing humidity of carrier gas at constant moisture of drift gas (7 ppm) and (B) increasing humidity of drift gas at constant moisture of carrier gas (18 ppm).

also detectable at constant drift times over the whole humidity range of the carrier gas. The signal intensities of these three peaks rise with increasing levels of humidity. These additional ions can be attributed to reactant ions with a higher degree of clustering. Because of the formation of these additional peaks, the signal intensity (peak heights and peak areas) of the main product ion peak at 5.3 ms decreases with increasing humidity.

In the case of enhanced drift gas humidity, considerable changes in drift times were observed. The drift time of negative reactant ions shifts from 5.3 to 5.7 ms with increasing humidity from 20 to 1800 ppm. In contrast, only a variation of ±0.01 ms was found within the same range of carrier gas humidity. These observations for the humid drift gas evidently result from the changing composition of the gas together with changes in the collisional cross section and different interaction forces being exerted on negative reactant ions and drift gas molecules. Although Figure 3B indicates decreasing peak heights with increasing humidity, it is notable that the peak area is nearly constant over the whole humidity range. This results from peak broadening, where the full width at half of the maximum level attained increases from 0.119 ms (19 ppm humidity) to 0.128 ms (2800 ppm). Unfortunately, the commonly used peak resolution (defined in IMS as resolving power = drift time/peak

dx.doi.org/10.1021/ac5007393 | Anal. Chem. 2014, 86, 5069–5076

width at half height) is an unsuitable parameter for characterizing this effect because of the shift to higher drift times and the simultaneous increase of full width at half-maximum. Furthermore, a considerable tailing of the reactant ion peak can be observed in both directions (lower and higher drift times). Both the peak broadening and the strong tailing of reactant ion peaks are attributable to further reactions taking place as the ions travel through the drift region. The two additional product ions found for humid carrier gases can also be identified within the spectrum. However, these ions appear with a very low relative abundance as broad peaks. The additional peak which was detected as shoulder of reactant ions peak in the case of humid carrier gas cannot clearly be assigned using the humid drift gas because of the considerable base width.

The influence of humidity on the blank ion mobility spectra can be summarized in the following way: Enhanced carrier gas humidity affects ionization reactions by forming additional ions, while higher levels of drift gas humidity lead to peak broadening and changes in drift behavior.

Drift Times of Halogenated Compounds. The spectra of 1-chlorohexane and 1-iodohexane are shown in Figure 4 as an example of the measurements carried out with dry gases, humid carrier gas, and humid drift gas.

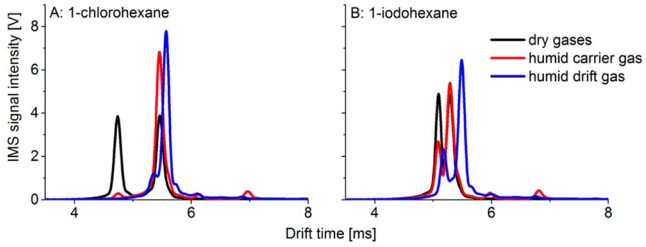

Figure 4. Ion mobility spectra of 10 nmol L^{-1} 1-chorohexane (A) and 0.5 nmol L^{-1} 1-iodohexane (B) measured with dry gases, humid carrier gas (1200 and 1220 ppm, respectively) and humid drift gas (1500 and 1790 ppm, respectively).

Under dry conditions, the drift time difference between the product ion peaks of chlorinated compounds (4.67 ms) and negative reactant ions (5.3 ms) is much more significant in comparison to 1-iodohexane (5.11 ms). These differences are in accordance with data from the literature, and result from ionic masses and the expected interactions between drift gas and product ions. All three chlorinated substances investigated achieved almost identical results. The product ion peaks of brominated compounds appear at 4.91 ms.

The drift times obtained with humid carrier gas are the same as those detected with dry gases. They are constant over the whole humidity range (see Figure 5). However, humid carrier gas causes the occurrence of additional product ions. These peaks appear at the same drift time as observed for blank measurements (Figure 3). It is notable that their intensity is not affected by the presence of chemical compounds. The intensity of these peaks increases with increasing humidity in the same way as measured for blank spectra. These additional peaks are not clearly observable in the case of humid drift gas.

Increasing drift gas moisture leads to longer drift times (Figure 5). However, these changes in peak position vary considerably for chlorinated, brominated and iodinated substances. Within a range from approximately 20 ppm humidity to 1800 ppm, the shift in drift time of $Cl^-(H_2O)_x$

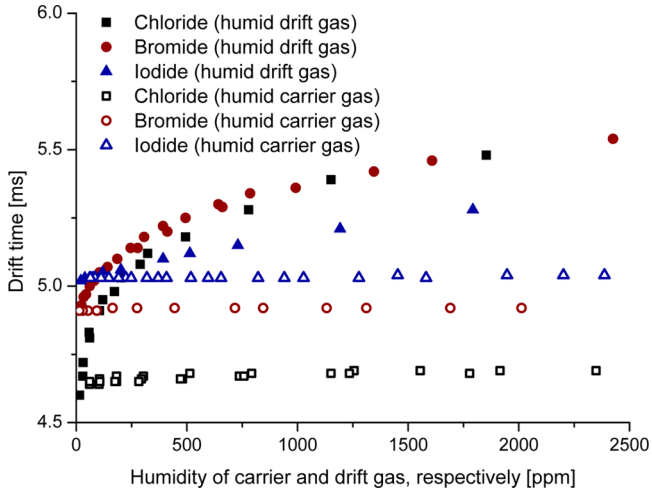

Figure 5. Drift time-shift of product ions formed from 1-chlorohexane, 1-bromohexane and 1-iodohexane with increasing humidity of carrier gas (with constant humidity of approximately 20 ppm of drift gas) and drift gas (with constant humidity of approximately 20 ppm of carrier gas).

product ions is 0.88 ms, for $Br^-(H_2O)_x$ product ions it is 0.57 ms, while only a difference of 0.26 ms was found for $I^-(H_2O)_x$. Very high levels of drift gas humidity do therefore not permit a differentiation between $Cl^-(H_2O)_x$ and $Br^-(H_2O)_x$ product ions, which is possible under dry conditions without any difficulty. Both peaks appear at comparable drift times as a shoulder of reactant ion peak. It is also notable that the drift time of $I^-(H_2O)_x$ ions under humid conditions is below that of chlorinated and brominated ions, although the opposite can be observed under dry conditions. The conclusion we can draw from this is that the shift in drift times dependent on drift gas humidity agrees with the expected changes in the composition of product ions. 1-iodohexane is comparatively unaffected by humidity and only minimal changes in clustering level x of the product ions $I^-(H_2O)_x$ can be expected. In contrast, product ions formed from chlorinated substances show a nonlinear dependence on humidity and the shift in drift times is much more significant.

The drift times detected for reactant ions shift in a similar way for each measurement depending on humidity of drift gas. Within a range between 20 and 1800 ppm humidity, the detectable drift time shifts from 5.3 to 5.7 ms. The different drift behavior of product ions and reactant ions therefore has an impact upon separating power, which is characterized in IMS as peak-to-peak resolution. These results are summarized in Table 1. As can be seen, the drift time differences between negative reactant ions and the product ions of 1-chlorohexane and 1-bromohexane decrease with increasing drift gas humidity; when humidity levels are above 2000 ppm, separation is almost impossible. Product and reactant ion peaks nearly merge at high humidity levels, although dry conditions allow a clear differentiation to be made with sufficient peak-to-peak resolution. Therefore, the drift time difference and the peak-to-peak resolution decrease. Since the shift of iodinated product ions is not as distinct as that of reactant ions, the drift time difference and peak-to-peak resolution improves with increasing humidity.

Changing drift times because of humidity of the supporting gases can generally result in the following effects: (1) influence on ionization processes, (2) varying interactions between

dx.doi.org/10.1021/ac5007393 | Anal. Chem. 2014, 86, 5069−5076

Table 1. Peak-to-Peak Resolution and Differences in Drift Times between Negative Reactant Ions and Product Ions of 1-Chlorohexane, 1-Bromohexane, and 1-Iodohexane Depending on Drift Gas Humidity[a]

1-chlorohexane			1-bromohexane			1-iodohexane		
humidity (ppm)	Δt_d (ms)	R_{pp}	humidity (ppm)	Δt_d (ms)	R_{pp}	humidity (ppm)	Δt_d (ms)	R_{pp}
21.6	0.63	2.63	23.9	0.33	1.36	21.1	0.19	0.80
35.9	0.56	2.41	32.6	0.33	1.40	39.1	0.20	0.84
63.5	0.50	2.22	61.3	0.32	1.31	59.2	0.23	0.95
104.3	0.45	1.92	116.4	0.30	1.23	119.0	0.25	1.08
184.3	0.40	1.74	182.4	0.28	1.17	202.4	0.28	1.24
283.3	0.36	1.57	300.9	0.24	0.98	392.5	0.30	1.31
466.8	0.31	1.18	499.0	0.21	0.81	513.3	0.30	1.30
757.9	0.25	0.85	764.8	0.19	0.73	730.8	0.31	1.26
1151.6	0.21	0.74	1234.4	0.18	0.59	1192.3	0.31	1.26
1763.0	0.12	0.50	1822.6	0.16	0.48	1792.5	0.31	1.25

[a] Δt_d = differences in drift time between negative reactant ions and negative product ions. R_{pp} = peak-to-peak resolution between negative reactant ions and negative product ions. R_{pp} = 2 × drift time difference of the two peaks/(peak width of peak 1 + peak width of peak 2)

product ions and drift gas molecules, and (3) further reactions of product ions during the traveling time through the drift tube.

The occurrence of product ion peaks at the same drift time under dry and humid conditions as well as the formation of additional product ions suggest that humid carrier gases cause changes in ionization processes. In contrast, varying drift gas humidity results in shifting drift time. This in turn is strongly dependent upon the properties of analytes, especially their tendency to form ion−water clusters. Therefore, these observations are clearly validated by the two reasons just mentioned. The lower drift velocity of $X^-(H_2O)_x$ product ions with increasing drift gas humidity can be attributed to more significant interactions taking place with the drift gas molecules, which contain a higher number of water molecules with increasing moisture. The occurrence of this effect can also be concluded from the blank measurements. The formation of ions with a different degree of clustering within the ion source enables clear differentiation of these peaks within the ion mobility spectrum. The gradual shift of drift times depending on the capability of product ions to attach water molecules is therefore evidence that a further clustering takes place within the drift tube as the substances travels through.

Quantitative Aspects. The influence of moisture on the quantitative determination of halogenated compounds was determined in two different ways: The concentration was held constant and the humidity of the supporting gases was increased. Furthermore, complete calibrations were acquired at certain moisture levels.

As shown in previous studies,[33] the general detectability of halogenated compounds depends on the nature of substituents and their bonding state. Regarding the halogenated *n*-hexanes, 1-iodohexane can be detected with the highest sensitivity, followed by 1-bromohexane, while 1-chlorohexane shows the lowest sensitivity. These findings result from decreasing bond energies in the order Cl > Br > I. The sensitivity of chlorinated compounds increases in the order vinyl compounds (trichloroethene) < alkyl compounds (1-chlorohexane) < benzyl chlorides. Alkyl chlorides and benzyl chlorides with a C−Cl bond to a sp^3 hybridized carbon atom showed enhanced sensitivities in comparison to trichloroethene, where the heterolysis of chlorine from the sp^2 hybridized carbon atom is evidently limited. However, trichloroethene contains three cleavable chlorine atoms and can therefore be detected with intensities which are close to 1-chlorohexane. These general observations were also found here be independently of the measuring conditions.

Enhanced humidity levels of the supporting gases generally result in reduced intensities. Due to the higher concentrations of water molecules within the ion source, less ionization reactions take place. The influence of enhanced moisture of the supporting gases is shown in Figure 6 (with benzyl chloride

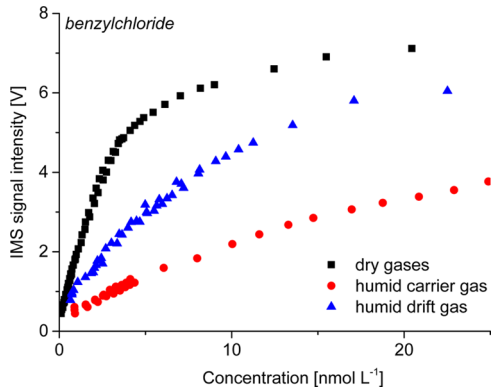

Figure 6. Comparison of calibration curves for benzyl chloride measured with dry gases, humid carrier gas, and humid drift gas. The humidity was approximately 800 ppm for each gas.

used as an example). As can be seen, humid carrier gas leads to a more significant reduction of the relative abundance of product ions formed in comparison to humid drift gas. This general observation holds true for nearly all substances investigated, although quantitative differences were found. This concurs with our results obtained by fluid dynamic calculation (Figure 1), where higher concentrations of water within the ion source were established if a humid carrier gas is applied. Furthermore, additional reactant ions are formed which do not take part in the ionization reaction. Therefore, less reactant ions are available for forming product ions in the scenario with the humid carrier gas.

The lowest influence of moisture on quantification was observed for 1-iodohexane. The calibrations at 800 ppm humidity show between 65 and 80% of the peak height for humid carrier gas and humid drift gas related to measurement with dry gases. Using humid carrier gas, the detectable intensities of 1-bomohexane and benzyl chloride are similar (within a range between 15 and 25%), while trichloroethene

dx.doi.org/10.1021/ac5007393 | Anal. Chem. 2014, 86, 5069−5076

and 1-chlorohexane appears with intensities below 6%. Recovery levels with humid drift gas are significantly greater for 1-bromohexane (40−50%), benzyl chloride (32−42%) and 1-chlorohexane (15−25%) and trichloroethene attains similar recoveries with humid drift gas compared to humid carrier gas.

Considering the measurements of constant concentrations and increasing humidity levels, a general reduction in product ion intensity can be observed for all compounds. The results are summarized in Figure 7. The impact of moisture agrees with

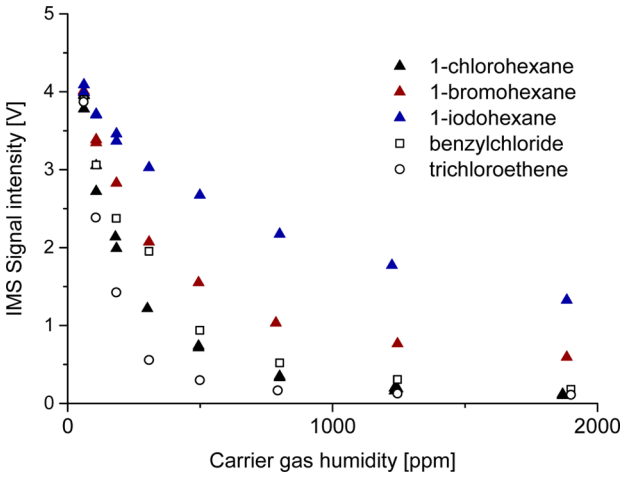

Figure 7. Dependence of signal intensity on the carrier gas humidity.

the general detectability. The intensities of 1-chlorohexane and trichloroethene decrease much more in comparison to the other substances. As can be seen from Figure 7, the influence of moisture is different for each compound and nonparallel correlations are obtained between the curves (intensity vs humidity) for each substance. These observations confirm our results achieved regarding the calibration curves.

An additional observation can be concluded from Figure 4A. While the intensity of product ions of chlorinated compounds decreases with increasing humidity of supporting gases, the peak height of reactant ions considerably increases. This effect is more significant when applying humid drift gas and is most pronounced for chlorinated compounds. A less significant increase of reactant ion intensity was observed during the measurements of 1-bromohexane, while only a slight increase was detected for 1-iodohexane. A general reason for this is that less product ions are formed with increasing moisture and less reactant ions are used for the ionization reaction. Therefore, the growth of reactant ion intensity concurs with reduced product ion intensity with increasing moisture (1-chlorohexane > 1-bromohexane > 1-iodohexane).

However, the significant increase of reactant ion peaks observed during measurement of the chlorinated compounds can also be caused by the formation of $Cl^-(H_2O)_x$ product ions with a higher number of water molecules. According to our calculations, the formation of $(H_2O)_2O_2^-$ and $(H_2O)_2Cl^-$ product ions can be expected in this humidity range. The ionic masses of 68 and 71 do not allow a separation from the ion mobility spectrum to be achieved.

Generally, the reduced detectability of halogenated substances with increasing humidity of carrier- and drift gases obviously results from a reduced formation of product ions within the ion source.

CONCLUSIONS

A main advantage of IMS is the detection of spectra that make it possible to recognize possible matrix effects. In contrast to other sensor techniques (which provide sum signals only), changes in ion mobility spectra clearly indicate increased moisture levels. A shift in the drift times of reactant ions can be used as an indicator for humid drift gases, while the occurrence of additional product ions shows that the injected sample gas stream contains too much moisture. These indicators are very important because of the influence of humidity on both peak assignment and quantification.

Generally, increased humidity levels within the spectrometer lead to lower quantitative results. Humid carrier gas has a more significant influence on quantification in comparison to humid drift gas, which additionally results in shifting of drift times.

The experimental setup, especially the flow system applied, allows separate investigations to be undertaken concerning the influence of humidity through both carrier and drift gases. Other flow systems, e.g. the traditional unidirectional flow system (where the sample gas stream is injected into the drift gas flow between ion source and shutter grid), lead to a mixing of both gases and the resulting influence of humidity can therefore affect results and create anomalies that differ from our observations due to the superimposing of both effects. However, the detectable impact on ion mobility spectra is the same as described above.

AUTHOR INFORMATION

Corresponding Author

*E-mail: helko.borsdorf@ufz.de.

Notes

The authors declare no competing financial interest.

REFERENCES

(1) Eiceman, G. A.; Stone, J. A. *Anal. Chem.* **2004**, *76*, 390a−397a.
(2) Koester, C. J.; Moulik, A. *Anal. Chem.* **2005**, *77*, 3737−3754.
(3) Baumbach, J. I. *Anal Bioanal Chem.* **2006**, *384*, 1059−1070.
(4) Karpas, Z.; Chaim, W.; Gdalevsky, R.; Tilman, B.; Lorber, A. *Anal. Chim. Acta* **2002**, *474*, 115−123.
(5) Chaim, W.; Karpas, Z.; Lorber, A. *Eur. J. Obstet. Gynecol. Reprod. Biol.* **2003**, *111*, 83−87.
(6) Budimir, N.; Weston, D. J.; Creaser, C. S. *Analyst* **2007**, *132*, 34−40.
(7) Lokhnauth, J. K.; Snow, N. H. *Anal. Chem.* **2005**, *77*, 5938−5946.
(8) Karimi, A.; Alizadeh, N. *Talanta* **2009**, *79*, 479−485.
(9) Bohrer, B. C.; Mererbloom, S. I.; Koeniger, S. L.; Hilderbrand, A. E.; Clemmer, D. E. *Annu. Rev. Anal Chem.* **2008**, *1*, 293−327.
(10) Burks, R. M.; Hage, D. S. *Anal Bioanal Chem.* **2009**, *395*, 301−313.
(11) Kanu, A. B.; Hill, H. H. *Talanta* **2007**, *73*, 692−699.
(12) Yinon, J. *TrAC, Trends Anal. Chem.* **2002**, *21*, 292−301.
(13) Johnson, P. V.; Beegle, L. W.; Kim, H. I.; Eiceman, G. A.; Kanik, I. *Int. J. Mass Spectrom.* **2007**, *262*, 1−15.
(14) Borsdorf, H.; Mayer, T.; Zarejousheghani, M.; Eiceman, G. A. *Appl. Spectrosc Rev.* **2011**, *46*, 472−521.
(15) Borsdorf, H.; Eiceman, G. A. *Appl. Spectrosc Rev.* **2006**, *41*, 323−375.
(16) Eiceman, G. A.; Karpas, Z. *Ion Mobility Spectrometry*, 2nd ed.; CRC Press: Boca Raton FL, 2005.
(17) Shvartsburg, A. A. *Differential Ion Mobility Spectrometry: Nonlinear Ion Transport and Fundamentals of FAIMS*, 1st ed.; CRC Press: Boca Raton, FL, 2008.
(18) Gutierrez-Osuna, R. *IEEE Sens. J.* **2002**, *2*, 189−202.
(19) Gurlo, A.; Riedel, R. *Angew. Chem.* **2007**, *119*, 3900−3923.

(20) Rock, F.; Barsan, N.; Weimar, U. *Chem. Rev.* **2008**, *108*, 705−725.
(21) Tabrizchi, M. *Appl. Spectrosc.* **2001**, *55*, 1653−1659.
(22) Borsdorf, H.; Mayer, T. *Talanta* **2012**, *101*, 17−23.
(23) Tabrizchi, M. *Talanta* **2004**, *62*, 65−70.
(24) Davis, E. J.; Dwivedi, P.; Tam, M.; Siems, W. F.; Hill, H. H. *Anal. Chem.* **2009**, *81*, 3270−3275.
(25) Tabrizchi, M.; Rouholahnejad, F. *J. Phys. D: Appl. Phys.* **2005**, *38*, 857−862.
(26) Tabrizchi, M.; Rouholahnejad, F. *Talanta* **2006**, *69*, 87−90.
(27) Erikson, H. A. *Phys. Rev.* **1928**, *32*, 791−794.
(28) Vautz, W.; Sielemann, S.; Baumbach, J. I. *Anal. Chim. Acta* **2004**, *513*, 393−399.
(29) Vautz, W.; Ruszany, V.; Sielemann, S.; Baumbach, J. *Int. J. Ion Mobility Spectrom* **2004**, *7*, 3−8.
(30) Bocos-Bintintan, V.; Brittain, A.; Thomas, C. L. P. *Analyst* **2001**, *126*, 1539−1544.
(31) Makinen, M.; Sillanpaa, M.; Viitanen, A. K.; Knap, A.; Makela, J. M.; Puton, J. *Talanta* **2011**, *84*, 116−121.
(32) Eiceman, G. A.; Karpas, Z.; Hill, H. H. *Ion Mobility Spectrometry*, 3rd ed.; Taylor & Francis Group: Boca Raton, FL, 2013.
(33) Borsdorf, H.; Mayer, T. *Talanta* **2011**, *83*, 815−822.
(34) Bork, N.; Kurten, T.; Enghoff, M. B.; Pedersen, J. O. P.; Mikkelsen, K. V.; Svensmark, H. *Atmos Chem. Phys.* **2011**, *11*, 7133−7142.
(35) Moruzzi, J. L.; Phelps, A. V. *J. Chem. Phys.* **1966**, *45*, 4617−&.
(36) Curtiss, L. A.; Melendres, C. A.; Reed, A. E.; Weinhold, F. *J. Comput. Chem.* **1986**, *7*, 294−305.
(37) Lee, E. P. F.; Dyke, J. M.; Wilders, A. E.; Watts, P. *Mol. Phys.* **1990**, *71*, 207−215.